

Role of Chain Transfer Agents in Free Radical Polymerization Kinetics

T. Furuncuoğlu, İ. Uğur, İ. Değirmenci, and V. Aviyente*

Chemistry Department, Boğaziçi University, 34342, Bebek, Istanbul, Turkey

Received July 7, 2009; Revised Manuscript Received January 6, 2010

ABSTRACT: This study deals with modeling the propagation and the chain transfer reactions in the free radical polymerization of ethylene, methyl methacrylate (MMA), and acrylamide (AM). The chain transfer agents modeled in the free radical polymerization of ethylene are the experimentally widely used species such as ethylene, methane, ethane, propane, trimethylamine, dimethylamine, chloroform, and carbon tetrachloride. The role of 4-X-thiophenols as chain transfer agents in the polymerization of MMA and AM has been investigated. Geometry optimizations have been carried out with the B3LYP/6-31+G(d) methodology. Reaction rate constants are calculated via the standard transition-state theory with the B3LYP/6-311+G(3df,2p)//B3LYP/6-31+G(d), MPWB1K/6-311+G(3df,2p)//B3LYP/6-31+G(d), and M05-2X/6-311+G(3df,2p)//B3LYP/6-31+G(d) methodologies, which reproduce qualitatively the experimental trends for the chain transfer rate constants. The usage of simple continuum models with the MPWB1K/6-311+G(3df,2p)//B3LYP/6-31+G(d) methodology for the solvation energies has slightly improved the accurate prediction of the chain transfer constants. Polar interactions highly influence the barrier heights for chain transfer reactions in the FRP of ethylene, MMA, and AM. Calculated chain transfer rate constants in the FRP of MMA and AM correlate quite well with the Hammett constants.

Introduction

The molecular weight control of polymers is a subject of increasing interest because many of their properties such as physical and mechanical properties depend on the chain length.¹ In the conventional free radical polymerization, the control of the polymer chain length is difficult to attain. The classical method of controlling molecular weight is the addition of chain transfer agents to the polymerization medium. For many industrially important systems, a chain transfer agent is added to the polymerization composition to lower the polymer molecular weight.² A growing macroradical abstracts a hydrogen atom from the chain transfer agent, giving a terminated polymer chain and a new initiating radical, which adds to the monomer giving a new propagating species. The general chain transfer constant, C_s , defined as the ratio of the chain transfer and propagation rate coefficients, k_{ct}/k_p , is a measure of the reactivity of a chain transfer agent. The higher C_s , the lower the concentration of the chain transfer agent required for a particular molecular weight reduction.³

$$C_s = \frac{k_{ct}}{k_p}$$

The decrease in the molecular weight by the addition of a chain transfer agent is quantitatively given by the Mayo equation,⁴ which expresses the reciprocal of the polymerization degree (D_{pn}) as a function of the rate of the chain growth and the chain stopping

$$\frac{1}{D_{pn}} = \frac{1 + \alpha}{(D_{pn})_0} + C_s \frac{[CTA]}{[M]}$$

In this equation, $(D_{pn})_0$ is the polymerization degree in the absence of chain transfer agent, [CTA] is the concentration of the chain transfer agent, [M] is the monomer concentration, and α is the fraction of termination by disproportionation.⁵

In the past decade, the control of molecular weight has also been achieved by a living radical polymerization such as atom transfer radical polymerization (ATRP),^{6–9} nitroxide-mediated polymerization (NMP),^{10,11} and reversible addition–fragmentation chain transfer (RAFT) polymerization.^{12,13} Catalytic chain-transfer (CCT) agents also have a control on the molecular weight: substituted cobalt porphyrins or benzoporphyrins have been shown to provide dramatic reductions in the molecular weight of the methacrylate polymers during radical polymerization with little to no reduction in the overall yield of polymer.¹⁴

In parallel to experimental developments, quantum mechanical tools have been used to model the chain transfer reactions in free radical polymerization processes. Radom et al. have used the B3LYP/6-31G(d) methodology and the curve-crossing model to study the hydrogen transfer between ethyl radical and ethylene: an example where kinetics does not follow thermodynamics.¹⁵ Gilbert et al. have modeled the short-chain branching in polyethylene with *ab initio* quantum mechanics up to the QCISD(T) level.¹⁶ Density functional calculations are reported for the bond dissociation energy of a number of dithioacetates, $CH_3C(S)S-R$ and selected dithiobenzoates, $PhC(S)S-R$, used mainly in addition–fragmentation transfer (RAFT) controlled radical polymerization.¹⁷ The usage of quantum chemical tools in elucidating the chain transfer process via the RAFT polymerization has been thoroughly investigated by Coote et al.¹⁸ The latter have identified significant penultimate effects in the equilibrium constants between active and dormant species of atom transfer radical systems (ATRP).¹⁹ The same group has determined the equilibrium constants for the Cu-based ATRP for a wide range of

*Corresponding author. E-mail: aviye@boun.edu.tr.

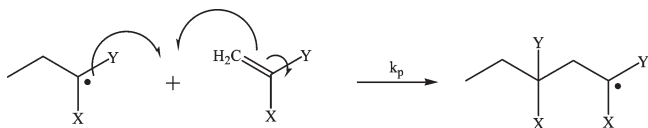
ligands and initiators in acetonitrile²⁰ and has reported the thermodynamic and electrochemical properties of alkyl halides used as ATRP initiators.²¹ Among others, a high-level ab initio study by the group of Coote et al. is on the evaluation of rate coefficients for the intra- and intermolecular hydrogen abstraction reactions in the formation of the various types of defect structures in radical suspension polymerization of vinyl chloride,²² followed by a study on PVC, where hydrogen abstraction reactions, especially backbiting and abstraction from chloroallylic end groups, are emphasized.²³ The main reaction routes that lead to the formation of structural defects in PVC have also been studied by Van Speybroeck et al. with the BMK/6-311+G(3df,2p)//B3LYP/6-31+G(d) methodology.²⁴ A DFT modeling study in our group has shown the chain transfer to play a major role in inhibiting the polymerization of dimethylaminoethyl acrylate.²⁵

Experimental and theoretical studies on hydrogen and halogen atom transfer reactions have illustrated the structure–reactivity relationship in these reactions as well as the importance of polar effects in the transition states; several theoretical frameworks such as the curve-crossing model of Shaik and Pross have been developed to explain these results.²⁶ A study on alkyl halides, RX, reports their reduction to the corresponding alkanes, RH, by triethylsilane in the presence of a suitable initiator and an alkanethiol catalyst.²⁷ The reactions of methanethiyl radicals (CH₃S•) with the cyclic anhydrides of glycine, alanine, sarcosine, and the acyclic peptides were studied by means of B3LYP/6-311+G(d,p) calculations, and it has been concluded that the ultimate site of free-radical damage in proteins will rest at the backbone α C-site rather than at a thiol.²⁸ Recently, high-level ab initio calculations have been used to understand the hydrogen abstraction by carbon-centered radicals from thiols where a reasonable correlation between the barrier height and the polar effects has been found.²⁹ Dolbier et al. have highlighted the importance of transition-state polar effects in hydrogen atom transfer reactions: the rate of reduction of fluoroalkyl radicals by PhSH has shown that PhS-H, a very efficient H atom donor to hydrocarbon radicals, reduced perfluoro-*n*-alkyl radicals 500 times slower. This result indicates that transition-state polar effects must also play a significant role in such hydrogen atom transfer reactions.³⁰

In this study, quantum mechanical calculations have been used to model and understand the role of chain transfer agents in the free radical polymerization of ethylene, methylmethacrylate (MMA), and acrylamide (AM).

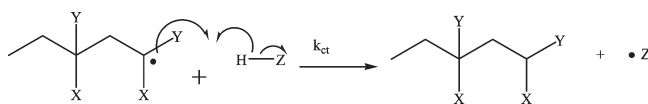
Methodology and Computational Procedure

The free-radical polymerization proceeds via a chain mechanism and consists of four elementary reactions, that is, initiation, propagation, chain transfer, and termination.³¹ The first step is the production of free radicals from the initiator molecule by light or heat. The initiator radical attacks the monomer to create a new radical. Successive additions of newly formed radicals and monomers is called propagation, which is the main reaction of polymerization.

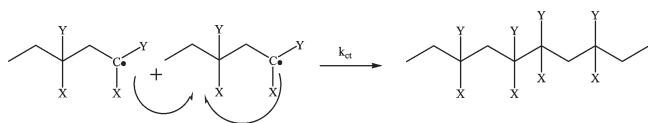


The propagating radical may attack another monomer by chain transfer, and the radical center may be transferred to

another chain, so that the molecular weight of the propagating polymer can be controlled.



The polymerization reaction ends up by the combination of two radicals.



The activated complex theory pictures a reaction between A and B as proceeding through the formation of an activated complex, C[‡], in a rapid pre-equilibrium



The activated complex falls apart by a unimolecular decay into the products, P.

Provided that \bar{K}^{\ddagger} is the equilibrium constant (despite one mode of C[‡] having been discarded), ΔG^{\ddagger} can be expressed through the definition

$$\Delta G^{\ddagger} = -RT \ln \bar{K}^{\ddagger}$$

Then, the rate constant becomes

$$k_2 = \kappa \frac{kT}{h} \frac{RT}{p^{\theta}} e^{-\Delta G^{\ddagger}/RT}$$

where k represents Boltzmann's constant, T is the temperature, h is Planck's constant, ΔG^{\ddagger} represents the molecular Gibbs free energy difference between the activated complex and the reactants (with inclusion of zero point vibrational energies), R is the universal gas constant, κ is the transmission coefficient, which is assumed to be ~ 1 , and p^{θ} is the standard pressure 10⁵ Pa (1 bar).³²

Density functional theory was used for all geometry optimizations by using the Gaussian 03 program package.³³ We selected the B3LYP/6-31+G(d) methodology as a cost-effective method because it was also used in previous reports to model the free radical propagation reactions.^{25,34–36} Although B3LYP is accurate for geometry optimizations, it is not suitable for obtaining kinetic results.³⁷ Different hybrid meta GGA functionals, MPWB1K³⁸ and M05-2X,³⁹ have been used to obtain more realistic kinetic results. A recent study on hybrid meta DFT methods has shown that MPWB1K can be used with confidence for a combination of thermochemistry, thermochemical kinetics, hydrogen bonding, and weak interactions, especially for thermochemical kinetics and noncovalent interactions.³⁸ M05-2X is a hybrid meta exchange-correlation functional that was designed for very general purposes such as kinetics, thermochemistry of main group elements, noncovalent interactions, ionization potentials, and activation energies.³⁹ For the activation energy barriers, it was found that this method is less accurate than BB1K, PWB6K, MPWB1K, MPW1K, BMK, for H-abstraction reactions but more accurate than B3LYP and other functionals.³⁹

The transition structures for the addition, hydrogen abstraction, and chlorine abstraction reactions have a very low vibrational frequency, corresponding to the internal rotation of the incoming radical about the forming bond. Recent studies of

radical addition^{25,35,40} and hydrogen abstraction reactions⁴¹ have been modeled by using the 1D-HR approach. In this study we used a mixed harmonic oscillator/hindered rotor (HO/HR) model in which all internal motions except the internal rotations corresponding to bond formation are approximated as independent harmonic oscillators. Tunneling corrections for the abstraction of hydrogen have been used in modeling because the abstracted hydrogen atom is light and its wavelength is large compared with the barrier width, thereby enabling it to “tunnel” through the barrier. Hybrid DFT methods such as MPW1K and B3LYP have been used to obtain reasonable estimates of the tunneling coefficients to within a factor of two to three.⁴² In recent studies, both Wigner⁴³ and Eckart⁴⁴ methodologies have been used successfully for hydrogen abstraction reactions.^{25,45}

To calculate the bond dissociation energies of the chain transfer agents, we have made use of isodesmic reactions that conserve the number of each bond type on either side of the reaction, resulting in significant improvements in calculated reaction enthalpies because of the cancellation of systematic calculation errors.⁴⁶

The bond dissociation energy for R-X (X = H or Cl) can be calculated by using eq 2



$$\text{BDE}(\text{R-X}) = \Delta_f H_{298}^0(\text{R}\cdot) + \Delta_f H_{298}^0(\text{X}\cdot) - \Delta_f H_{298}^0(\text{R-X}) \quad (2)$$

The energy of the isodesmic reaction 3 has been expressed in eq 4



$$\Delta_{\text{rxn}} H_{298}^0(3) = \Delta_f H_{298}^0(\text{CH}_3\text{X}) + \Delta_f H_{298}^0(\text{R}\cdot) - \Delta_f H_{298}^0(\text{CH}_3\cdot) - \Delta_f H_{298}^0(\text{R-X}) \quad (4)$$

Equation 4 is substituted in eq 2 to evaluate the bond dissociation energy of R-X, as displayed in eq 5

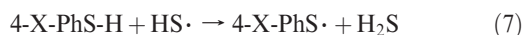
$$\text{BDE}(\text{R-X}) = \Delta H_{\text{rxn}}(3) - \Delta_f H_{298}^0(\text{CH}_3\text{X}) + \Delta_f H_{298}^0(\text{CH}_3\cdot) + \Delta_f H_{298}^0(\text{X}) \quad (5)$$

where $\Delta_f H_{298}^0(\text{CH}_3\text{Cl}) = -19.57 \text{ kcal mol}^{-1}$,⁴⁷ $\Delta_f H_{298}^0(\text{CH}_4) = -17.78 \text{ kcal mol}^{-1}$,⁴⁷ $\Delta_f H_{298}^0(\text{CH}_3\cdot) = 35.05 \text{ kcal mol}^{-1}$,⁴⁸ $\Delta_f H_{298}^0(\text{Cl}) = 29.03 \text{ kcal mol}^{-1}$,⁴⁸ and $\Delta_f H_{298}^0(\text{H}) = 52.10 \text{ kcal mol}^{-1}$ have been used.⁴⁸

Similarly, for the reaction



the isodesmic reaction



has been utilized to determine the bond dissociation energy of 4-X-PhS-H as

$$\text{BDE}(4\text{-X-PhS-H}) = \Delta H_{\text{rxn}}(7) - \Delta_f H_{298}^0(\text{H}_2\text{S}) + \Delta_f H_{298}^0(\text{HS}\cdot) + \Delta_f H_{298}^0(\text{H}\cdot) \quad (8)$$

where $\Delta_f H_{298}^0(\text{H}_2\text{S}) = -4.94 \text{ kcal mol}^{-1}$, $\Delta_f H_{298}^0(\text{HS}\cdot) = 34.20 \text{ kcal mol}^{-1}$, and $\Delta_f H_{298}^0(\text{H}) = 52.10 \text{ kcal mol}^{-1}$ have been used.⁴⁸

In this study, the propagation of ethylene, the chain transfer reactions of ethylene with various chain transfer agents, and the

propagation of MMA and AM and their chain transfer reactions have been modeled with the B3LYP/6-311+G(3df,2p)//B3LYP/6-31+G(d), MPWB1K/6-311+G(3df,2p)//B3LYP/6-31+G(d), and M05-2X/6-311+G(3df,2p)//B3LYP/6-31+G(d) methodologies. Calculations are carried out at 403.15 K for the free radical polymerization of ethylene, whereas those of MMA and AM are carried out at 298.15 K. In the case of 4-X-thiophenols, the effect of a polar environment was taken into account by the use of the self-consistent reaction field (SCRf) theory, utilizing the integral equation formalism-polarizable continuum (IEF-PCM) model in solution.⁴⁹ Each solute molecule is embedded in a cavity surrounded by the relevant dielectric continuum; terms for the nonelectrostatic contributions of the solvent, such as dispersion, repulsion, and cavitation are also included. The solvent was taken to be acetonitrile in the free radical polymerization of MMA and water in the free radical polymerization of AM, as described experimentally.¹ At each level of theory (LOT), free energies of each species in solution were obtained as the sum of the corresponding gas-phase free energy, the calculated free energy of solvation with nonelectrostatic effects, and a correction term, $RT \ln(24.46)$, to take account of the fact that the solvation energy is computed for the passage from 1 mol L⁻¹(g) to 1 mol L⁻¹(soln).⁵⁰

Results

I. Modeling the Chain Transfer Process in the Free Radical Polymerization of Ethylene. A. Propagation of Ethylene.

Experimental and quantum chemical studies on the chain length dependency of the propagation rate constant of ethylene have been widely carried out.³⁵ Olaj et al. observed a slight decrease in k_p in terms of chain length.⁵¹ Willemse showed that k_p is only dependent on the chain length in the oligomeric range,⁵² but this point of view has been later rejected by Olaj et al.⁵³ The latter claim that a long-range chain length dependence of k_p extends over several hundreds of propagation steps. The effect of extending the chain length of the radical on the calculated frequencies of the transitional modes in the addition of *n*-alkyl radicals to ethylene was investigated by Radom et al.⁵⁴ Another computational study about the free radical polymerization of ethylene indicated that the propagation rate coefficient has largely converged to within a factor of 1.3 by the hexyl radical stage, although a weaker chain-length dependence is detected that extends far beyond the oligomeric range.³⁵ A study of chain length effects in the free-radical polymerization of vinyl chloride and acrylonitrile indicated that rate coefficients had largely converged to their long chain limit in the dimer radical stage.⁵⁵ The results from applying the pulsed laser photolysis method to styrene polymerization are consistent with other recent work indicating that the value of k_p for styrene is chain-length-dependent at least for chain lengths of three units.⁵⁶

The propagation of ethylene considered in this study is displayed in Scheme 1. The hexyl radical is used as the growing chain to model the propagation and the chain transfer reactions. A relaxed potential energy scan study has shown that along the propagation reaction the hexyl radical approaches the ethylene molecule in the gauche geometry ($\tau = 57.38^\circ$). The reaction barriers for the addition of various gamma-substituted propyl radicals to alkenes were obtained via ab initio molecular orbital calculations:⁵⁷ in each case, the lowest energy transition structure conformations were those for gauche-addition transition structures in which the monomer substituent was close to both the gamma substituent of the propyl radical and the unpaired electron. As can be seen from the potential surface energy

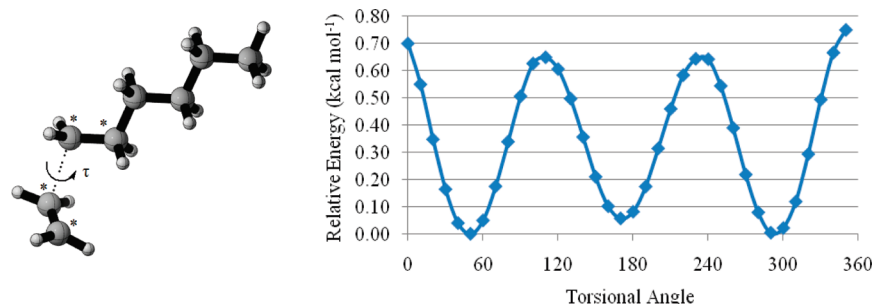
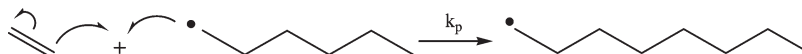


Figure 1. Transition state and potential energy scan along τ for the propagation reaction of ethylene (B3LYP/6-31+G(d)).

Scheme 1. Mechanism for the Propagation Reaction of Ethylene

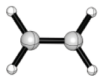
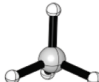
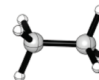
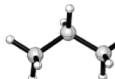
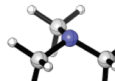
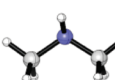
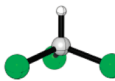
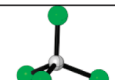


scan, the eclipsed conformations in the polymer chain are $\sim 0.70 \text{ kcal mol}^{-1}$ less stable than the gauche conformations (Figure 1). This type of conformation has already been observed in the free radical propagation reaction of acrylates and methacrylates.^{25,34,37}

B. Chain Transfer in the Propagation of Ethylene. In this study, the substituent effect, the steric effect, the unsaturation, and the presence of heteroatoms on the transfer process of H(X) with a polyethylene growing chain are analyzed. This approach will elucidate how different chain transfer agents control the growing chain in the free radical polymerization of ethylene. It is known that halomethanes, which include chloroform, carbon tetrachloride, carbon tetrabromide, and bromotrichloromethane, have been widely used as CTA (telogens) for the preparation of telomers.⁵⁸ The perhalomethanes (e.g., carbon tetrachloride, carbon tetrabromide, and bromotrichloromethane) react in the chain transfer process to exchange a halogen atom and form a perhaloalkyl radical that initiates a new propagating chain. The low C_s value for chloroform as compared with the one of carbon tetrachloride is explained by the strength of the C–H bond in the former. The enhancement of chain transfer reactivity has been postulated to occur by stabilization of the respective transition states for the transfer reactions by contributions from polar effects.⁵⁹ The experimental results displayed in Table 1 reveal the fact that the electron-rich amine derivatives as well as chloromethanes increase the chain transfer constant along the polymerization of polyethylene.

The chain transfer reactions along the polymerization of ethylene have been modeled by taking into account all of the possible reaction mechanisms during the abstraction of the labile atom of the chain transfer agents by the hexyl radical (Scheme 2). There is one possible chain transfer mechanism for ethylene, methane, ethane, and trimethylamine because the hydrogen atoms are equivalent. On the other hand, propane and dimethylamine possess two different types of H atoms. In the case of chloroform, there is one labile hydrogen atom and three environmentally similar chlorine atoms; in the case of carbon tetrachloride as a chain transfer agent, a chlorine atom is transferred to the hexyl radical. Note that the overall rate constant has been taken to be calculated in all cases, and symmetry has not been taken into account by symmetry numbers in the partition functions; instead, in the case of C_2H_6 , the rate constant for the abstraction of a H atom is multiplied by six. For CHCl_3 , the overall rate constant includes the rate constant for H-atom abstraction, three times the rate constant for Cl

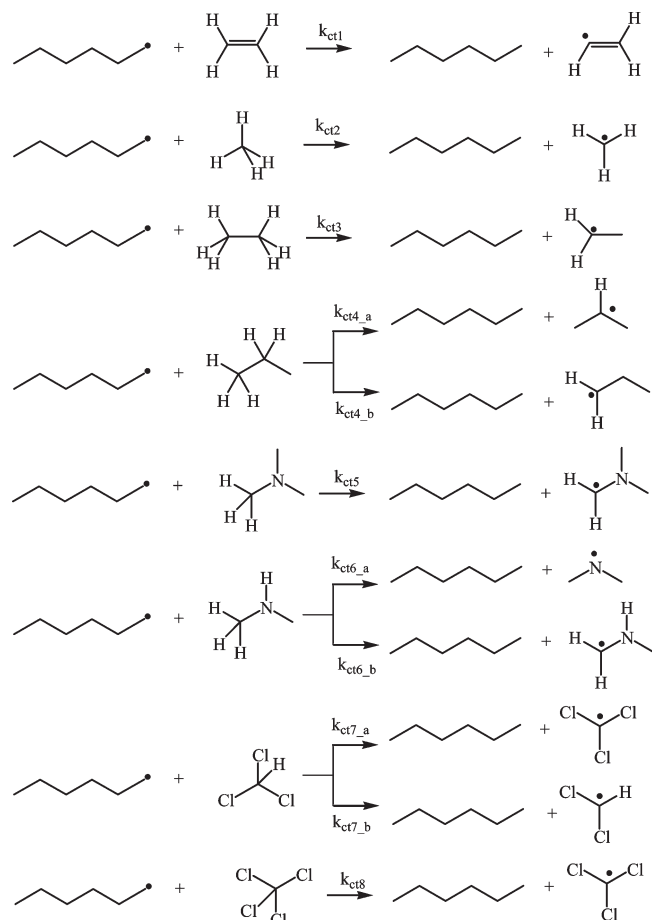
Table 1. Chain Transfer Agents Used in the Polymerization of Ethylene (C_s Is the Experimental Chain Transfer Constant)

Chain transfer agent			C_s [60]
1	Ethene		1.00E-05
2	Methane		1.00E-04
3	Ethane		6.00E-04
4	Propane		2.70E-03
5	Trimethylamine		1.80E-02
6	Dimethylamine		1.90E-01
7	Chloroform		2.90E-01
8	Carbon tetrachloride		9.80E-01

abstraction, and so on. A similar procedure was followed in a study of H-abstraction by OH radicals where the total rate constant was considered to be the sum of the individual rate constants.⁶¹

The 3D structures for the transition states of the chain transfer reactions are gathered in Figure 2. TS-PE-1 is a late transition state in which a hydrogen atom of ethylene is abstracted by a hexyl radical; in this structure, the breaking carbon–hydrogen bond is longer than the forming carbon–hydrogen bond. The hydrogen atom transfer reaction of

Scheme 2. Chain Transfer Reactions along the Polymerization of Ethylene



methane (TS-PE-2), ethane (TS-PE-3), and propane (TS-PE-4b) show similar transition-state structures with linear C—X—C features. TS-PE-3 and TS-PE-4b have equal breaking and forming bond distances because of the similarity of the electronic environment on both sides. The electron donor substituents facilitate the H-abstraction, and their transition states (TS-PE-5, TS-PE-6a, and TS-PE-6b) are early. In the case of chloroform, the hydrogen atom (TS-PE-7a) migrates faster than Cl (TS-PE-7b). The favorable long-range Cl \cdots H interactions in CHCl₃ probably inhibits the rupture of the C—Cl bond as compared with the one in CCl₄, where all four bonds are equivalent (Table 2).

The mechanistic details of the chain transfer process in the free radical polymerization of ethylene have been analyzed in detail (Table 3). Ethylene being a very stable molecule is not a good chain transfer agent; the chain transfer reaction is endothermic, and this is justified by the value of its BDE. Consideration of methane and ethane as chain transfer agents reveals the fact that the addition of a methyl group in ethane decreases the barrier by ~ 2 kcal mol⁻¹, whereas the heat of the reaction alters by almost 4.5 kcal mol⁻¹ because of the electron donor methyl group. The additional methyl group in isopropane facilitates the H-abstraction similarly; however, in *n*-propane, the end methyl group does not assist the H-abstraction reaction, and *n*-propane behaves like ethane. The enthalpies of activation of the amine derivatives are lower compared with the ones of the hydrocarbons because of the presence of the electron donor group; Hammond's postulate is obeyed as reflected in the exothermicity of these chain transfer reactions. Among the chloro-

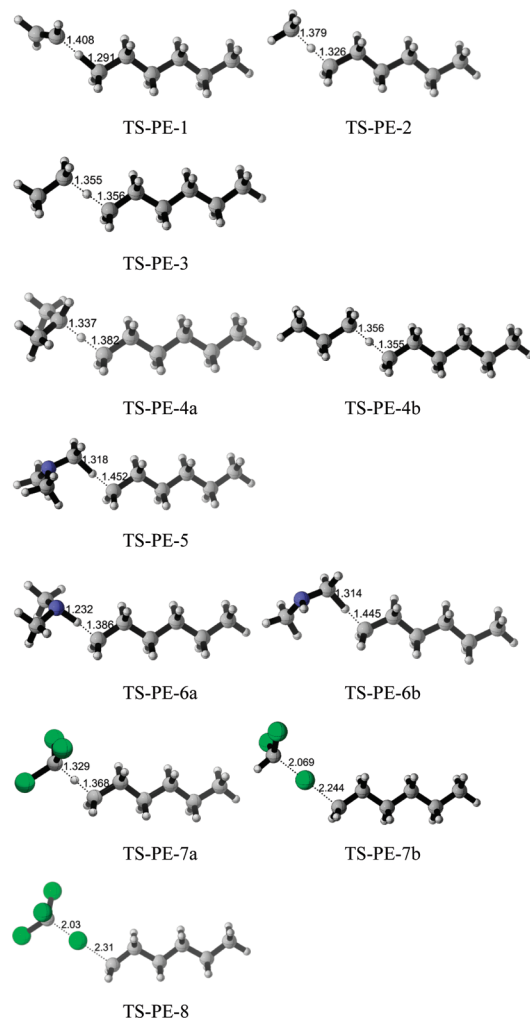


Figure 2. Transition states of the chain transfer reactions in the propagation of ethylene (B3LYP/6-31+G(d)).

Table 2. Activation Barriers, E_a (kcal·mol⁻¹), for the Chain Transfer Reactions in the FRP of Ethylene (MPWB1K/6-311+G(3df,2p)//B3LYP/6-31+G(d))

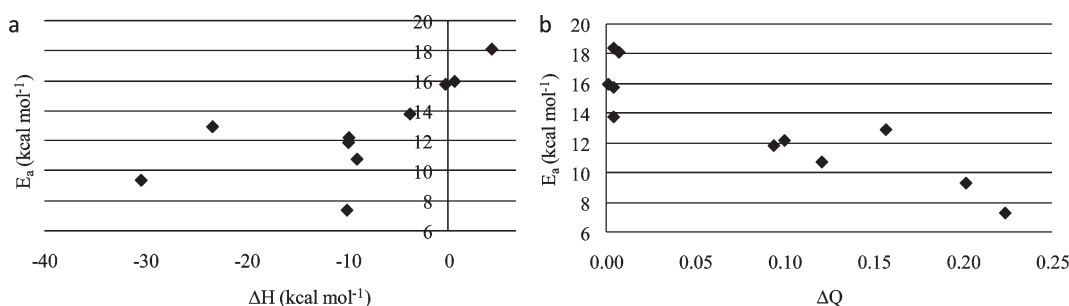
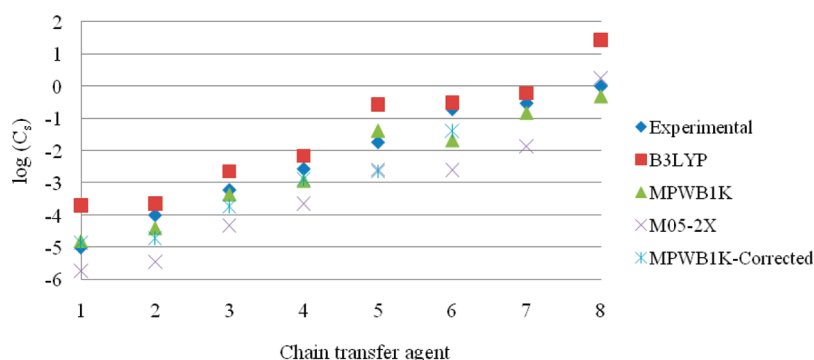
	chain transfer agent	TS	E_a
1	ethene	TS-PE-1	18.44
2	methane	TS-PE-2	18.16
3	ethane	TS-PE-3	15.79
4	propane	TS-PE-4a	13.80
		TS-PE-4b	16.00
5	trimethylamine	TS-PE-5	12.22
6	dimethylamine	TS-PE-6a	10.77
		TS-PE-6b	11.88
7	chloroform	TS-PE-7a	7.34
		TS-PE-7b	12.95
8	carbon tetrachloride	TS-PE-8	9.35

methanes, chlorine abstraction from CCl₄ is easier than the others; CCl₃—Cl has the lowest BDE, as determined experimentally.^{21,62} Nevertheless, as seen from the barrier heights, H abstraction is easier than chlorine abstraction probably because of its smaller size, and CHCl₃ acts as a chain transfer agent preferentially via its H. The hydrogen abstraction by carbon-centered radicals from chloroalkanes and amines is generally an exothermic process, in which a strong C—H bond is formed at the expense of weaker bonds broken. There is a correlation between the barrier height and the reaction enthalpy, and the Evans–Polanyi rule somewhat rule holds for these reactions (Figure 3a).

Table 3. Forward Barrier ($\Delta H_{\text{fwd}}^{\ddagger}$), Reverse Barrier ($\Delta H_{\text{rev}}^{\ddagger}$), Enthalpy (ΔH), Charge–Transfer Energies ($\text{C}_6\text{H}_{13}^+\text{AR}^-$ and $\text{C}_6\text{H}_{13}^-\text{AR}^+$), and NBO Charges (Q) on the Hexyl Group the Chain Transfer Agents in the Transition Structures (A = H or Cl)^{a,b,c}

R-H	$\Delta H_{\text{fwd}}^{\ddagger}$	$\Delta H_{\text{rev}}^{\ddagger}$	ΔH	$\text{C}_6\text{H}_{13}^+\text{AR}^-$	$\text{C}_6\text{H}_{13}^-\text{AR}^+$	$Q(\text{C}_6\text{H}_{13})$	$Q(\text{R})$	BDE
$\text{CH}_2\text{CH-H}$	18.06	8.92	9.14	6.22	9.90	−0.092	−0.096	109.84 (110.7) ^d
$\text{CH}_3\text{-H}$	17.40	13.09	4.32	6.58	13.61	−0.097	−0.104	104.94 (104.99) ^d
$\text{CH}_3\text{CH}_2\text{-H}$	15.40	15.65	−0.25	6.64	11.84	−0.105	−0.101	100.38 (101.1) ^d
$(\text{CH}_3)_2\text{CH-H}$	13.64	17.42	−3.78	6.72	11.18	−0.109	−0.105	96.86 (98.6) ^d
$\text{CH}_3\text{CH}_2\text{CH}_2\text{-H}$	15.74	15.10	0.64			−0.104	−0.105	101.27
$(\text{CH}_3)_2\text{NCH}_2\text{-H}$	12.08	21.89	−9.81	6.81	7.77	−0.146	−0.046	90.86
$(\text{CH}_3)_2\text{N-H}$	10.49	19.50	−9.01	6.79	8.27	−0.09	−0.211	91.72
$\text{CH}_3\text{NHCH}_2\text{-H}$	11.67	21.52	−9.85			−0.142	−0.048	90.80
$\text{CCl}_3\text{-H}$	7.43	17.43	−10.00	7.53	10.91	0.145	−0.079	90.78 (95.8) ^e
$\text{CHCl}_2\text{-Cl}$	13.01	36.32	−23.31			0.136	−0.021	93.99 (77.8) ^e
$\text{CCl}_3\text{-Cl}$	9.45	39.82	−30.37	8.23	11.02	−0.011	−0.213	87.07 (84.27) ^f

^a Barriers and enthalpies are calculated at 403.15 K (kcal mol^{-1}); bond dissociation energies are calculated at 298.15 K; NBO charges are obtained from the MPWB1K/6-311+G(3df,2p) wave function calculated on the B3LYP/6-31+G(d) geometry. ^b Last column displays the Bond Dissociation Energies (kcal mol^{-1}) (MPWB1K/6-311+G(3df,2p)//B3LYP/6-31+G(d)). ^c C_6H_{13} (radical) IE = 8.17 eV, EA = 0.52 eV. ^d Refs 46–48. ^e Ref 62. ^f BDE of $\text{CH}_3\text{COOC}(\text{H})(\text{CH}_3)\text{-Cl}$ has been calculated as 84.23 kcal mol^{-1} in ref 21.

**Figure 3.** (a) Reaction barrier versus reaction enthalpy (MPWB1K/6-311+G(3df,2p)//B3LYP/6-31+G(d)) and (b) reaction barrier versus charge separation between the hexyl radical and the chain transfer agent (MPWB1K/6-311+G(3df,2p)//B3LYP/6-31+G(d)).**Figure 4.** $\log(C_s)$ against chain transfer agent in the FRP of ethylene (Table 4).

The relative energies of the charge-transfer configurations at the transition structure have been modeled by considering the relative energies of the $\text{C}_6\text{H}_{13}^+\text{AR}^-$ and $\text{C}_6\text{H}_{13}^-\text{AR}^+$ using the charge transfer energies between the isolated C_6H_{13} and the chain transfer agents. “A” is H for the first nine species and is Cl for the last two species in Table 3. The hexyl radical (C_6H_{13}) is the propagating radical; the $\text{C}_6\text{H}_{13}^+\text{AR}^-$ configuration is modeled as the difference of the (vertical) ionization energy of the C_6H_{13} radical and (vertical) electron affinity of the AR fragment, whereas the $\text{C}_6\text{H}_{13}^-\text{AR}^+$ configuration is modeled as the difference of the (vertical) ionization energy of AR and (vertical) electron affinity of the C_6H_{13} fragment. The $\text{C}_6\text{H}_{13}^+\text{AR}^-$ species are lower in energy than the $\text{C}_6\text{H}_{13}^-\text{AR}^+$ species, confirming the charge transfer to the chain transfer agent. The amount of charge transferred to the agent exceeds the one on the alkyl fragment in most cases, as expected. There is a reasonable correlation between the activation energy and the charge separation in the transition structures reflecting the increasing ability of

charge-transfer stabilization in the transition state: CCl_4 with the lowest barrier has the highest charge difference, ΔQ (Figure 3b).

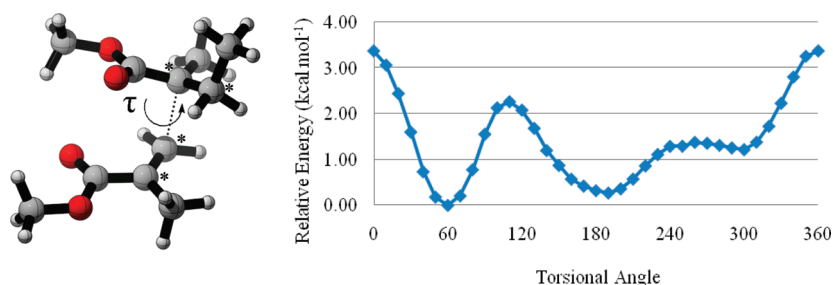
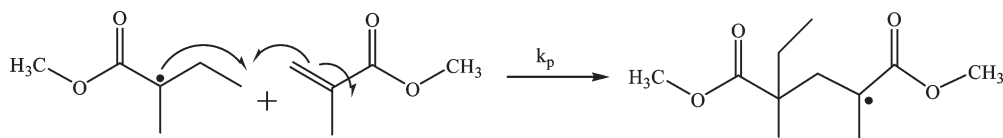
C. Level of Theory Study. The methodology used has been tested and an LOT study has been performed on the chain transfer constant, C_s , for the free radical polymerization of ethylene with the MPWB1K, B3LYP, and M05-2X methodologies. All functionals used reproduce qualitatively quite well the experimental trend; the results with the MPWB1K functional have the smallest mean unsigned error (MUE) for the chain transfer constants, C_s , as depicted in Figure 4 (Table 4).

II. Modeling the Chain Transfer Process in the Free Radical Polymerization of Methylmethacrylate and Acrylamide (AM). *A. Propagation of MMA.* The free radical polymerization of MMA is modeled, as depicted in Scheme 3. PMMA is resistant to many chemicals but soluble in organic solvents such as ketones, chlorinated hydrocarbons, and esters. Optical clarity is the main feature of this plastic. In many

Table 4. LOT Study on the Chain Transfer Constants (C_s) for the Various Chain Transfer Agents in the FRP of Ethylene (403.15 K)^a

chain transfer agent	C_s (exptl) ^b	C_s (calcd)			
		B3LYP	MPWB1K	M05-2X	MPWB1K ^c
1 ethene	1.00×10^{-5}	1.98×10^{-4}	1.53×10^{-5}	1.83×10^{-6}	1.39×10^{-5}
2 methane	1.00×10^{-4}	2.27×10^{-4}	3.90×10^{-5}	3.59×10^{-6}	1.96×10^{-5}
3 ethane	6.00×10^{-4}	2.32×10^{-3}	4.30×10^{-4}	4.83×10^{-5}	1.89×10^{-4}
4 propane	2.70×10^{-3}	6.90×10^{-3}	1.14×10^{-3}	2.25×10^{-4}	1.29×10^{-3}
5 trimethylamine	1.80×10^{-2}	2.69×10^{-1}	4.14×10^{-2}	2.58×10^{-3}	2.25×10^{-3}
6 dimethylamine	1.90×10^{-1}	3.14×10^{-1}	2.09×10^{-2}	2.50×10^{-3}	4.08×10^{-2}
7 chloroform	2.90×10^{-1}	6.09×10^{-1}	1.48×10^{-1}	1.34×10^{-2}	2.34
8 carbon tetrachloride	9.80×10^{-1}	2.80×10^1	4.90×10^{-1}	1.76	1.15×10^{-2}
MUE		3.47	0.10	0.16	0.03
R^2		0.91	0.97	0.90	1.00
STDEV		3.24	0.03	0.21	0.00087

^a k_p ($C_6H_{13}^\bullet$)(B3LYP/6-311+G(3df,2p)//B3LYP/6-31+G(d)) = $4.74 \text{ L mol}^{-1} \text{ s}^{-1}$; (MPWB1K/6-311+G(3df,2p)//B3LYP/6-31+G(d)) = $4.09 \times 10^2 \text{ L mol}^{-1} \text{ s}^{-1}$; (M05-2X/6-311+G(3df,2p)//B3LYP/6-31+G(d)) = $1.03 \times 10^5 \text{ L mol}^{-1} \text{ s}^{-1}$. ^b Ref 60. ^c Corrected with HIR and Eckart tunneling corrections.

**Figure 5.** Transition state and potential energy scan along τ for the propagation reaction of MMA (B3LYP/6-31+G(d)).**Scheme 3. Mechanism for the Propagation Reaction of MMA**

applications, it is an excellent substitute for glass; it has good mechanical properties as well.⁶³

As already known experimentally and demonstrated computationally, the syndiotactic polymer is preferred over the isotactic one.³⁴ A conformational analysis has been carried out for the syndiotactic propagating radical chain (Figure 5). The most stable conformer has been found to be the one with $\tau = 60.12^\circ$, and the gauche addition is preferred as in the propagation of ethylene; however, notice the height of the rotational barrier due to steric effects, almost $3.5 \text{ kcal mol}^{-1}$, as opposed to the one in the propagation of ethylene. The global minimum of this transition structure is stabilized by long-range $\text{H} \cdots \text{O}$ interactions ($-\text{O}-\text{H}_2\text{C}-\text{H} \cdots \text{O}=\text{C}-$). The propagation rate constant, k_p , for the lowest energy conformer has been considered in the calculation of C_s .

B. Chain Transfer Reaction in MMA. The addition of thiophenols to the polymerization of MMA in organic media is known to reduce considerably the polymer molecular weight without variations in the polymerization rate (Scheme 4).¹ The data collected for 4-X-thiophenols have shown that k_{ct} was markedly dependent on the 4-substituent; the higher rate constant was obtained for the thiophenol bearing the strong electron donor amino group.

For the transition states, the potential energy scan along the critical bond ($\text{S}-\text{H} \cdots \text{C}^\bullet$) has been performed for $\text{X} = \text{H}$, and the global minimum is found to correspond to the dihedral angle $\text{C}-\text{S} \cdots \text{C}-\text{C}(\text{C}=\text{O})$ having a value of 96.20° ; all of the other transition structures follow this trend.

The lengths of the forming and breaking bonds in the transition states are a consequence of the electronic nature of the substituents at position 4; for example, the more electron donor the substituent, the shorter the breaking bond, and the longer the forming bond, the earlier is the transition state (Figure 6). Also notice that as the electron-donation capacity of the substituent increases, the difference between the forming and breaking bond distances increases. The greatest difference is observed when the substituent is an amino group because of its higher electron donation capability (Figure 6).

C. Propagation of AM. Polyacrylamide (PAM) and the copolymers of PAM have received considerable attention because they reached large-scale industrial use such as wastewater treatment, soil erosion control, cosmetic additive, drug design, and so on.^{65–69}

Tacticity control of AM has been attained by using Lewis acid or polar compound additives and polar solvents, which can strongly interact with the amide groups via coordination or hydrogen bonding interaction to influence the stereochemistry during the propagation and increase the isotacticity of the polymer (Scheme 5).⁷⁰ A detailed conformational search along the formation of the critical bond for the propagation of the isotactic acrylamide (Figure 7) has shown that the structure with the dihedral $\tau = 106.95^\circ$ corresponds to the global minimum for this transition state. Also notice that this structure has an intramolecular hydrogen bond between the hydrogen (H), bonded to the nitrogen atom of

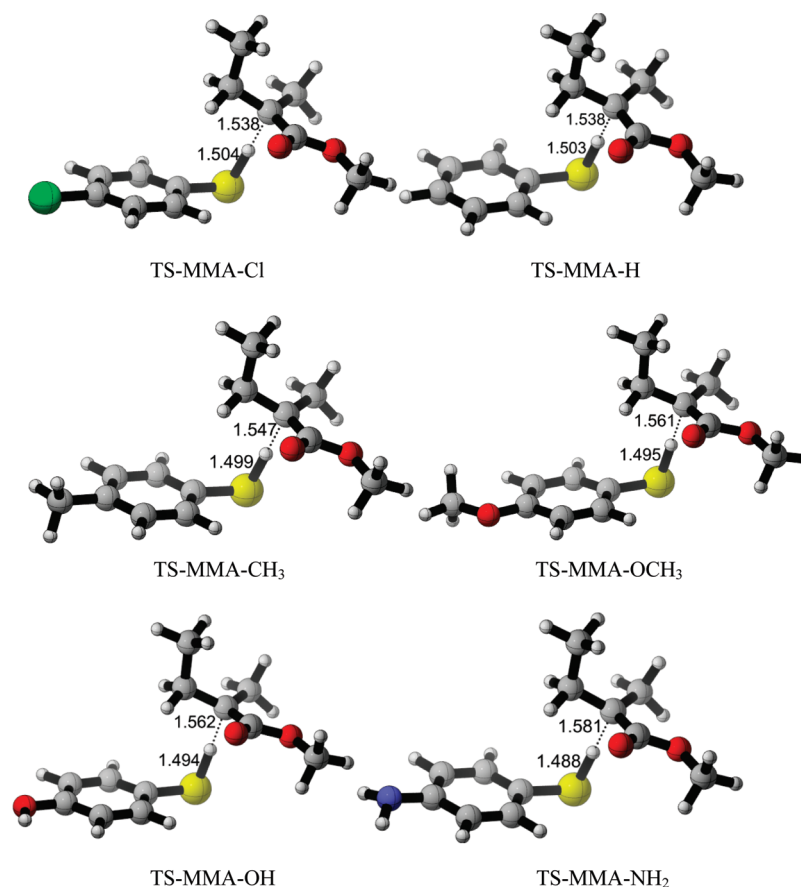
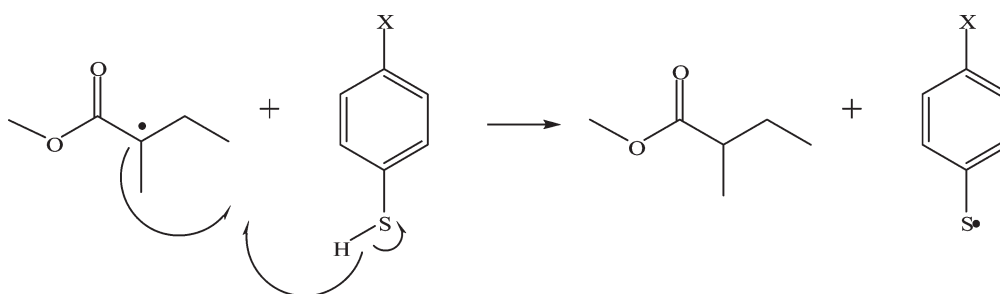


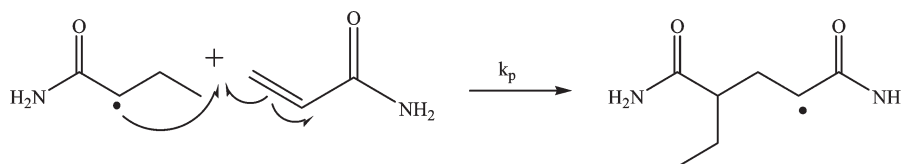
Figure 6. Transition states for the chain transfer reactions in the FRP of MMA (B3LYP/6-31+G(d)).

Scheme 4. Chain Transfer Reaction between 4-X-Thiophenols and MMA^a



^a X = Cl, H, CH₃, OCH₃, OH, NH₂.

Scheme 5. Mechanism for the Propagation Reaction for AM



radical moiety, and the oxygen (O) of the monomer with a close contact of 2.03 Å. The propagation rate constant, k_p , for this lowest energy conformer has been considered for all calculations.

D. Chain Transfer Reaction in AM. The chain transfer process from AM has been modeled based on the reaction in Scheme 6.

The global minimum for TS-AM-H corresponds to the structure with a torsional angle C-S...C-C(CH₂-CH₃) of 170.88°. This structure is stabilized by the interaction

between the positively charged hydrogen atom (0.410) bonded to nitrogen in the radicalic moiety and the closest negatively charged carbon atom (−0.114) in the thiophenol ring (Figure 8).

The highest chain transfer constant in the polymerization of AM, as in MMA, is achieved with 4-NH₂-thiophenol bearing the strong electron-donor group NH₂.

The hydrogen abstraction by the monomer radicals (MMAR and AMR) from 4-X-thiophenols is an exothermic process in which a strong C–H bond is formed and a weak

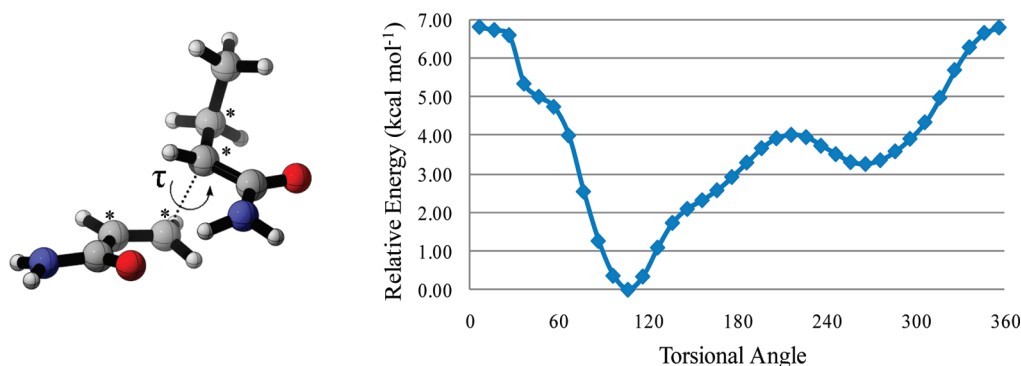
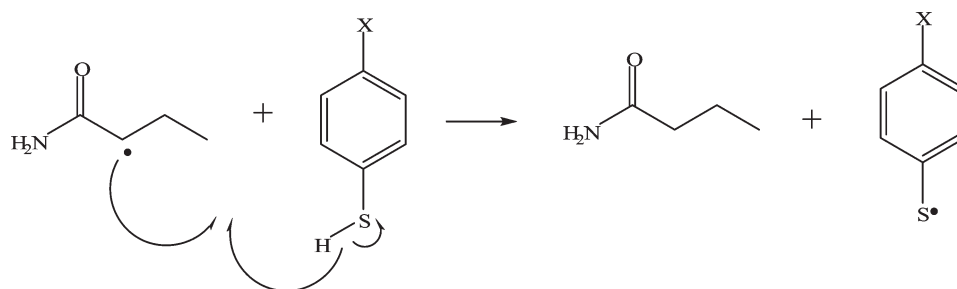


Figure 7. Transition state and potential energy scan along τ for the propagation reaction of AM (B3LYP/6-31+G(d)).

Scheme 6. Chain Transfer Reaction between 4-X-Thiophenols and AM^a



^a X = H, NHCOCH₃, CH₃, OCH₃, OH, NH₂.

Table 5. Forward Barrier ($\Delta H^\ddagger_{\text{fwd}}$), Reverse Barrier ($\Delta H^\ddagger_{\text{rev}}$), Enthalpy (ΔH), Charge-Transfer Energies (R^+SR^- and R^-SR^+), and NBO Charges (Q) on the Alkyl and Thiyl Fragments in the Transition Structures for $\text{CH}_3\text{MMA}^\bullet + \text{HSPhX} \rightarrow \text{CH}_3\text{MMAH} + \cdot\text{SPhX}$ and $\text{CH}_3\text{AM}^\bullet + \text{HSPhX} \rightarrow \text{CH}_3\text{AMH} + \cdot\text{SPhX}$ (MPWB1K/6-311+G(3df,2p)//B3LYP/6-31+G(d))^a

MMA								
X	$\Delta H^\ddagger_{\text{fwd}}$	$\Delta H^\ddagger_{\text{rev}}$	ΔH	R^+SR^-	R^-SR^+	$Q(\text{alkyl})$	$Q(\text{thiyl})$	BDE
H	6.1	13.7	-7.6	6.92	9.19	-0.046	-0.118	79.4
Cl	5.7	13.8	-8.2	7.32	9.15	-0.041	-0.125	78.8
CH ₃	5.6	14.4	-8.8	6.95	8.88	-0.052	-0.111	78.2
OCH ₃	5.2	15.9	-10.7	7.00	9.21	-0.054	-0.108	76.2
OH	4.7	15.4	-10.7	7.05	9.46	-0.056	-0.108	76.2
NH ₂	4.6	17.6	-13.1	6.89		-0.062	-0.098	74.5
AM								
X	$\Delta H^\ddagger_{\text{fwd}}$	$\Delta H^\ddagger_{\text{rev}}$	ΔH	R^+SR^-	R^-SR^+	$Q(\text{alkyl})$	$Q(\text{thiyl})$	BDE
H	3.7	16.7	-13.0	7.48	9.12	-0.015	-0.137	79.4
NHCOCH ₃	2.9	18.4	-15.5	7.65	8.63	-0.020	-0.130	76.9
CH ₃	3.2	17.5	-14.2	7.51	8.85	-0.018	-0.132	78.2
OCH ₃	2.8	18.9	-16.1	7.55	9.17	-0.030	-0.117	76.2
OH	2.4	18.5	-16.1	7.61	9.43	-0.032	-0.114	76.2
NH ₂	2.2	20.7	-18.5	7.44		-0.029	-0.118	74.5

^a Barriers and enthalpies are calculated at 298.15 K (kcal mol⁻¹); NBO charges are obtained from the MPWB1K/6-311+G(3df,2p) wave function calculated with B3LYP/6-31+G(d).

S-H bond is broken. The BDEs of MMA (89.6 kcal mol⁻¹) and AM (95.1 kcal mol⁻¹) are higher than the BDEs of the S-H bond dissociation energies (Table 5). This is in agreement with a study on hydrogen abstraction from thiols by carbon-centered radicals²⁹ and also with a study on biologically relevant systems where hydrogen transfer from a thiol to a carbon-centered radical could help to limit oxidative damage on proteins.²⁸ The reaction barriers are the lowest for the most electron donor groups: -OCH₃, -OH, and -NH₂. The S-H BDEs of thiols fall into a relatively narrow range despite the wide variation in the properties of the substituents, which can be explained in terms of the para location of the substituent insulating the substituent from the breaking S-H bond. To explore the effect of the various

descriptors used in the curve-crossing model of Shaik and Pross,²⁶ the reaction barriers have been plotted against the reaction enthalpy, the average singlet-triplet gap of the closed shells reactants and products, the energy for charge transfer between the isolated alkyl and thiyl fragments of the transition structures, and the difference in the charges on the alkyl and thiyl fragments of the transition structures. Charge transfer energies (electronvolts) were calculated as the difference in the vertical ionization energy of the donor species and the vertical electron affinity of the acceptor. R^+SR^- refers to charge transfer from the monomer-radical fragment to the thiyl fragment, whereas R^-SR^+ refers to charge transfer from the thiyl to the monomer radical.

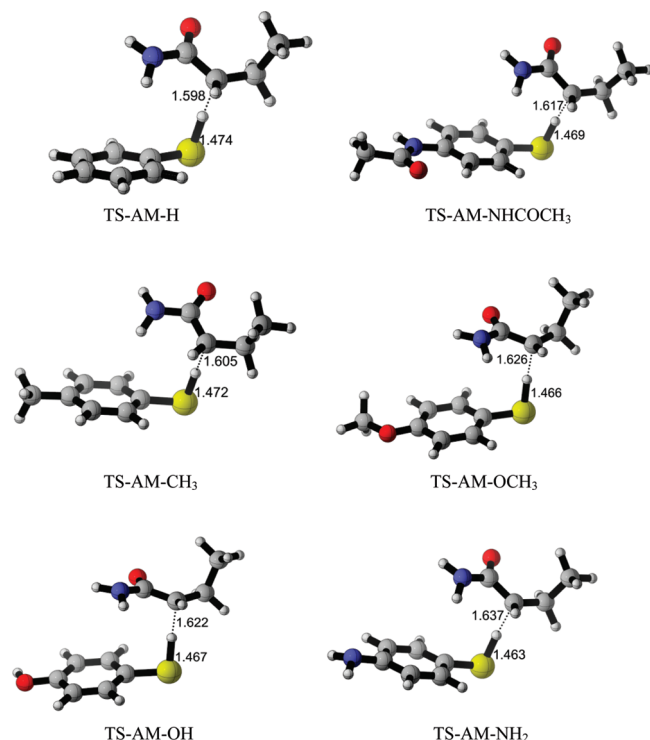


Figure 8. Transition states for the chain transfer reactions in the FRP of AM (B3LYP/6-31+G(d)).

Among these descriptors, a reasonable correlation between the barrier height and the reaction enthalpy obeying the Evans–Polanyi rule⁶⁴ has been determined, as displayed in Figure 9. In all cases, the preferred direction of charge transfer is from the alkyl radical to the thiyl radical. (The R^+SR^- configuration is preferred.) This finding is confirmed by the lower charge-transfer energies for the R^+SR^- configuration and also by the negative charges on the thiyl fragment in the transition structure. In general, the electron-donating groups on the thiyl radical increase the charge-transfer stabilization of the transition state and lower the barrier compared with the nonsubstituted case ($X = H$). Also notice that the degree of charge separation in the transition structures is more pronounced in the case of AM as compared with MMA, and this behavior is reflected in barrier lowering of the former.

These results suggest that polar interactions influence highly the barrier heights in hydrogen abstraction from thiols by $CH_3\text{-MMA}\cdot$ and $CH_3\text{-AM}\cdot$.

E. Level of Theory Study. The methodological study carried out for the FRP of ethylene has been repeated for the chain transfer rate constants of the reactions of 4-X-thiophenols with MMA and AM (Table 6, Figure 10). In the case of MMA, the MUE is similar with all methodologies; even though B3LYP yields the highest regression coefficient, the MPWB1K values lie closer to the normalized experimental values. For AM, the smallest MUE against the normalized experimental values has been reproduced with the B3LYP and MPWB1K methodologies. Nevertheless, as seen in Figure 10, B3LYP values are far away from the experimental ones.

Coote et al. have demonstrated that DFT methods fail to provide an accurate description of the energetics of radical reactions when compared with G3(MP2)-RAD benchmark values.⁷¹ In this study, even though accurate predictions of rate constants failed with DFT methodologies, as claimed in previous studies on radicals,^{71–73} reasonable agreement with

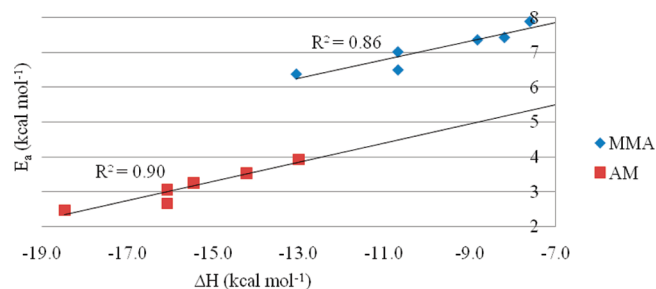


Figure 9. Reaction barrier versus reaction enthalpy (MPWB1K/6-311+G(3df,2p)//B3LYP/6-31+G(d)).

the experimental trends has been achieved with all three methodologies. Among the three methods tested, MPWB1K is found to have the best MUE values and R^2 values. M05-2X, which is found to have improved performance for energetics involving radicals, is performing equally well as MPWB1K, except for the low R^2 value in the case of MMA.⁷²

Tunneling corrections have been evaluated with Eckart's methodology. For H transfer reactions, these corrections are meaningful because there is no tunneling in the propagation reaction; its neglect in hydrogen transfer leads to a noncanceling error. Tunneling corrections increase the rate constants by approximately three and two orders of magnitude in the case of MMA and AM, respectively. (Detailed information is given in the Supporting Information.) HIR corrections amount to 2.31 for the propagation of MMA, whereas they are between 2 and 3 for the chain transfer reactions of MMA. Similarly, HIR corrections do not alter the C_s of AM because the correction factor is 1.09 for k_p and ~ 1.5 for k_{ct} . Overall, HIR corrections are seen to cancel each other in the case of C_s , whereas tunneling corrections for H-abstraction reactions increase the magnitude of C_s , and the experimental trend is reproduced with tunneling corrected C_s as well.

The effect of the solvent has been taken into account for the chain transfer constant, C_s , for 4-X-thiophenols with the MPWB1K/6-311+G(3df,2p)//B3LYP/6-31+G(d) methodology in water for AM and in acetonitrile for MMA. In the case of MMA (Figure 10), the experimental C_s values are very well matched for the first four 4-X-thiophenols ($X = Cl, H, CH_3$ and OCH_3); the discrepancy for the last two thiols ($X = OH$ and NH_2) can be attributed to the H-bonding capacity of the latter, which is not taken into account with the continuum model. Long-range interactions between the solvent, CH_3CN , and the substituents (OH and NH_2) are expected to take place, and explicit solvent molecules must be included to mimic the accurate experimental trend. In the case of the FRP of AM, specific solute–solvent interactions are expected not only between substituents and the solvent but also between the propagating polymer chain and its surroundings, and thus accurate description of the solvent is not to be expected with the continuum model. Nevertheless, note that the substituent effect is reproduced quite well with the continuum model (Figure 10).

Hammett Plots

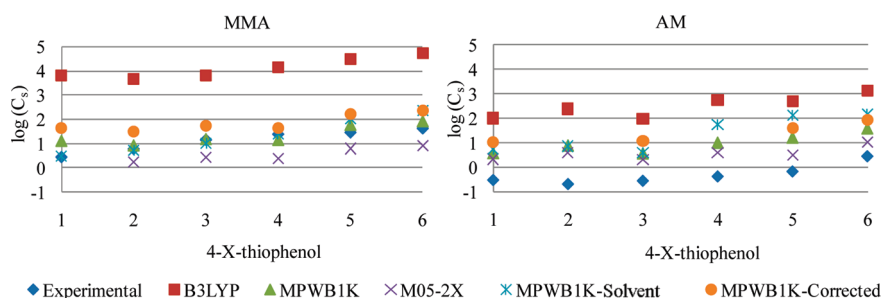
Hammett quantified the effect of substituents on any reaction by defining an empirical electronic parameter, σ , which is derived from the acidity constants of substituted benzoic acids. Therefore, the electronic substituent parameter, σ_X , for any substituent X is defined by

$$\sigma_X = \log \frac{K_X}{K_H}$$

Table 6. LOT Study on the Chain Transfer Rate Constants (k_{ct}) of 4-X-thiophenols in the FRP of MMA and AM (298.15 K)^a

			k_{ct} exptl [1]	k_{ct} calculated				
				B3LYP	MPWB1K	M05-2X	MPWB1K-(solution) ^b	MPWB1K ^c
MMA								
1	Cl	900	2.61×10^1	7.34×10^1	1.44×10^4	4.50×10^{-2}	6.07×10^2	
2	H	1900	1.85×10^1	4.81×10^1	8.20×10^3	7.74×10^{-2}	4.19×10^2	
3	CH ₃	4500	2.65×10^1	8.75×10^1	1.28×10^4	1.46×10^{-1}	7.01×10^2	
4	OCH ₃	7580	5.56×10^1	8.01×10^1	1.11×10^4	3.47×10^{-1}	6.09×10^2	
5	OH	8900	1.25×10^2	3.31×10^2	2.89×10^4	1.48	2.38×10^3	
6	NH ₂	13 100	2.13×10^2	4.64×10^2	3.74×10^4	3.13	3.17×10^3	
MUE			1.60	1.48	1.37	8.18	0.98	
R ²			0.86	0.77	0.70	0.81	0.76	
STDEV			1.78	1.92	0.87	7.78	1.52	
AM								
1	H	1150	4.78×10^2	1.57×10^3	2.23×10^5	7.26×10^{-2}	4.85×10^3	
2	NHCOCH ₃	800	8.45×10^2	1.46×10^3	1.33×10^5	9.27×10^{-2}		
3	CH ₃	1090	4.62×10^2	1.53×10^3	2.11×10^5	5.32×10^{-2}	5.37×10^3	
4	OCH ₃	1650	2.51×10^3	4.09×10^3	4.04×10^5	7.12×10^{-1}		
5	OH	2600	2.34×10^3	6.53×10^3	3.27×10^5	1.64	1.80×10^4	
6	NH ₂	10 900	5.94×10^3	1.52×10^4	1.10×10^6	1.81	3.87×10^4	
MUE			1.75	0.59	0.97	7.49	0.70	
R ²			0.89	0.95	0.96	0.58	0.93	
STDEV			1.60	0.86	0.34	8.06	0.94	

^a MMA [k_p (B3LYP/6-311+G(3df,2p)//B3LYP/6-31+G(d)) = $4.14 \times 10^{-3} \text{ L mol}^{-1} \text{ s}^{-1}$; (MPWB1K/6-311+G(3df,2p)//B3LYP/6-31+G(d)) = $5.87 \text{ L mol}^{-1} \text{ s}^{-1}$, (M05-2X/6-311+G(3df,2p)//B3LYP/6-31+G(d)) = $4.50 \times 10^3 \text{ L mol}^{-1} \text{ s}^{-1}$; (MPWB1K/6-311+G(3df,2p)//B3LYP/6-31+G(d)-acetonitrile) = $1.39 \times 10^{-2} \text{ L mol}^{-1} \text{ s}^{-1}$. AM [k_p (B3LYP/6-311+G(3df,2p)//B3LYP/6-31+G(d)) = $2.81 \times 10^5 \text{ L mol}^{-1} \text{ s}^{-1}$; (MPWB1K/6-311+G(3df,2p)//B3LYP/6-31+G(d)) = $4.09 \times 10^2 \text{ L mol}^{-1} \text{ s}^{-1}$; (M05-2X/6-311+G(3df,2p)//B3LYP/6-31+G(d)) = $1.04 \times 10^7 \text{ L mol}^{-1} \text{ s}^{-1}$; (MPWB1K/6-311+G(3df,2p)//B3LYP/6-31+G(d)-water) = $1.31 \times 10^{-2} \text{ L mol}^{-1} \text{ s}^{-1}$]. ^b Solvent is acetonitrile for MMA and water for AM. ^c Corrected with HIR and Eckart tunneling corrections.

Figure 10. $\log(C_s)$ versus 4-X-thiophenols in the FRP of MMA and AM (Table 6).

Where K_X and K_H are the acidity constants for the substituted benzoic acid and benzoic acid, respectively, in water at 25 °C. The σ value of a substituent is a measure of the electron-withdrawing or electron-releasing ability of that substituent compared with H. Therefore, it is possible to analyze substituent effects on the rate or equilibrium constants for other reactions. This is done by plotting the set of rate (or equilibrium) constants for a given reaction against the σ values of the substituents. The resulting correlations are expressed by

$$\sigma_p = \log \frac{k_X}{k_H}$$

for rate constants. These two equations are together known as the Hammett equations.⁷⁴

To examine the substituent effects on reactivity in chain transfer reactions of MMA and AM, calculated chain transfer rate constants (k_{ct}) have been plotted against the σ_p parameters (Table 7 and Figure 11).⁷⁵

According to Hammett plots for both experimental and calculated chain transfer rate constants, the rate of chain transfer agents is directly proportional to the electronic strength of the substituents. The σ_p values of 4-X-thiophenols with X being a weak electron donor substituent cause a slight deviation

Table 7. Hammett Substituent Constants (σ_p)⁷⁵

	σ_p
X	
Cl	0.22
H	0
NHCOCH ₃	0
CH ₃	-0.17
OCH ₃	-0.28
OH	-0.37
NH ₂	-0.63

from linearity. Therefore, by excluding 4-Cl-thiophenol and 4-NHCOCH₃-thiophenol from the Hammett plots of MMA and AM, respectively, linear relationships with $R^2 = 0.85$ and 0.92 are obtained.

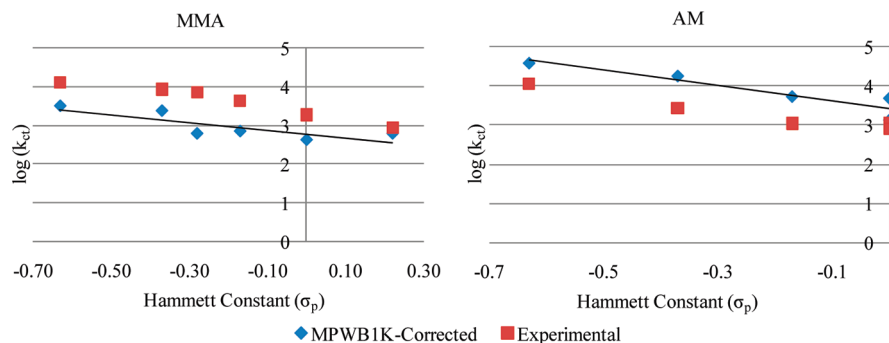


Figure 11. Hammett plots for calculated chain transfer rate constant (k_{ct}) values of MMA and AM (MPWB1K/6-311+G(3df,2p)//B3LYP/6-31+G(d)).

Experimentally, thiophenols are known to be better chain transfer agents than phenols in the FRP of MMA and AM.¹ Our calculations (B3LYP/6-31+G(d)) corroborate this finding: the chain transfer rate coefficient (k_{ct}) of thiophenol ($3.11 \times 10^2 \text{ L mol}^{-1} \text{ s}^{-1}$) is 28×10^3 times higher than that of phenol ($1.10 \times 10^{-2} \text{ L mol}^{-1} \text{ s}^{-1}$) in the FRP of MMA, and k_{ct} of thiophenol ($6.41 \times 10^3 \text{ L mol}^{-1} \text{ s}^{-1}$) is 3.5×10^3 times higher than that of phenol ($1.83 \text{ L mol}^{-1} \text{ s}^{-1}$) in the FRP of AM.

4-X-substituted thiophenols have higher k_{ct} values with MMA than with AM. This experimental observation is justified by our findings where $k_{ct}(\text{MMA}) > k_{ct}(\text{AM})$. This behavior is attributed to the higher rate of propagation of AM as compared with MMA: $k_p(\text{MMA}) = 5.87 \text{ L mol}^{-1} \text{ s}^{-1}$, whereas $k_p(\text{AM}) = 4.09 \times 10^2 \text{ L mol}^{-1} \text{ s}^{-1}$ with MPWB1K. As previously mentioned (Figure 7), the propagation of AM takes place via a transition structure stabilized by H-bonding causing acceleration of this propagation reaction.

Pulsed laser polymerization measurements of the homopropagation rate coefficients (k_p) for a series of para-substituted styrene monomers (4-X-styrene: X = OCH₃, CH₃, F, Cl, Br) at 20, 30, and 40 °C have been reported. The simple Hammett equation did not quantitatively describe the substituent effects on the k_p values of the series of para-substituted styrene monomers, although it provided a reasonable qualitative account of the trends in the data. The failure of the Hammett equations was probably due to the nonsystematic variation of the reaction constant because substituents on both reacting species were simultaneously altered.⁷⁶

The role of polar effects in the case of 4-X-thiophenols is confirmed by the strong correlations between the calculated rate constants and Hammett constants. This behavior is different than the one mentioned above because of the systematic variation of the substituent at the para position of the thiophenol ring altering the charge separation of the transition structure and the kinetics of the reaction.

Conclusions

In this study, the reactivity of chain transfer agents in the free radical polymerization of ethylene, MMA, and AM has been modeled with quantum chemical tools. The B3LYP/6-311+G(3df,2p)//B3LYP/6-31+G(d), MPWB1K/6-311+G(3df,2p)//B3LYP/6-31+G(d), and M05-2X/6-311+G(3df,2p)//B3LYP/6-31+G(d) methodologies have been tested against the experimental results to assess the level of theory. In all cases, the MPWB1K/6-311+G(3df,2p)//B3LYP/6-31+G(d) methodology is found to reproduce the experimental trend the best. In the case of polyethylene, chloromethanes and amines are found to control the polymerization better than alkanes and alkenes. In the case of MMA and AM, 4-X-thiophenols have higher chain transfer rate constants than their corresponding phenolic counterparts. The electron-releasing ability of the 4-X substituent is found to

accelerate the chain transfer process. The relationship between the electronic features of the substituent and the rate of chain transfer has been illustrated with Hammett plots. Overall, the models used in this study have proved to be adequate in the rationalization of the FRP kinetics. Similar calculations can be carried out with confidence to predict the characteristics of the chain transfer agent prior to experimental results.

Supporting Information Available: Cartesian coordinates, energies, activation barriers, preexponential factors, chain transfer rate constants, tunneling, and HIR corrections. This material is available free of charge via the Internet at <http://pubs.acs.org>.

Acknowledgment. The computational resources used in this work were provided by the TUBITAK ULAKBIM High Performance Computing Center, the Boğaziçi University Research Foundation (project 08M101), and the National Center for High Performance Computing of Turkey (UYBHM) under the grant number 20502009. I.D. acknowledges the sixth framework project COSBIOM (FP6-2004-ACC-SSA-2.517991) for funding the travel and lodging expenses to the conference DFT07 (Amsterdam), where part of this article was presented. Special thanks are due to Dr. Mehmet Demirörs (Dow Chemicals) for initiating this study.

References and Notes

- (1) Valdebenito, A.; Encinas, M. V. *Polymer* **2005**, *46*, 10658–10662.
- (2) Valdebenito, A.; Encinas, M. V. *J. Photochem. Photobiol., A* **2008**, *194*, 206–211.
- (3) Heuts, J. P. A.; Davis, T. P.; Russell, G. T. *Macromolecules* **1999**, *32*, 6019–6030.
- (4) Mayo, F. R. *J. Am. Chem. Soc.* **1943**, *65*, 2324–2329.
- (5) *Polymer Handbook*, 4th ed.; Brandrup, J., Immergut, E. H., Grulke, E. A., Eds.; Wiley-Interscience: Hoboken, NJ, 1999.
- (6) Wang, J. S.; Matyjaszewski, K. *J. Am. Chem. Soc.* **1995**, *117*, 5614–5615.
- (7) Patten, T. E.; Xia, J.; Abernathy, T.; Matyjaszewski, K. *Science* **1996**, *272*, 866–868.
- (8) Matyjaszewski, K.; Xia, J. *Chem. Rev.* **2001**, *101*, 2921–2990.
- (9) Kamigaito, M.; Ando, T.; Sawamoto, M. *Chem. Rev.* **2001**, *101*, 3689–3745.
- (10) Georges, M. K.; Veregin, R. P. N.; Kazmaier, K. M.; Hamer, G. K. *Macromolecules* **1993**, *26*, 2987–2988.
- (11) Hawker, C. J.; Bosman, A. W.; Harth, E. *Chem. Rev.* **2001**, *101*, 3661–3688.
- (12) Chiefari, J.; Chong, Y. K.; Ercole, F.; Krstina, J.; Jeffery, J.; Le, T. P. T.; Mayadunne, R. T. A.; Meijs, G. F.; Moad, C. L.; Moad, G.; Rizzardo, E.; Thang, S. H. *Macromolecules* **1998**, *31*, 5559–5562.
- (13) Goto, A.; Sato, K.; Tsujii, Y.; Fukuda, T.; Moad, G.; Rizzardo, E.; Thang, S. H. *Macromolecules* **2001**, *34*, 402–408.
- (14) Gridnev, A. A.; Ittel, S. D. *Chem. Rev.* **2001**, *101*, 3611–3659.
- (15) Heuts, J. P. A.; Pross, A.; Radom, L. *J. Phys. Chem.* **1996**, *100*, 17087–17089.

- (16) Toh, J. S. S.; Huang, D. M.; Lovell, P. A.; Gilbert, R. G. *Polymer* **2001**, *42*, 1915–1920.
- (17) Matyjaszewski, K.; Poli, R. *Macromolecules* **2005**, *38*, 8093–8100.
- (18) (a) Izgorodina, E. I.; Coote, M. L. *Macromol. Theory Simul.* **2006**, *15*, 394–403. (b) Coote, M. L.; Krenske, E. H.; Izgorodina, E. I. *Macromol. Rapid Commun.* **2006**, *27*, 473–497.
- (19) Lin, C. Y.; Coote, M. L.; Petit, A.; Richard, P.; Poli, R.; Matyjaszewski, K. *Macromolecules* **2007**, *40*, 5985–5994.
- (20) Tang, W.; Kwak, Y.; Braunecker, W.; Tsarevsky, N. V.; Coote, M. L.; Matyjaszewski, K. *J. Am. Chem. Soc.* **2008**, *130*, 10702–10713.
- (21) Lin, C. Y.; Coote, M. L.; Gennaro, A.; Matyjaszewski, K. *J. Am. Chem. Soc.* **2008**, *130*, 12762–12774.
- (22) Purmova, J.; Pauwels, K. F. D.; Van Zoelen, W.; Vorenkamp, E. J.; Schouten, A. J. *Macromolecules* **2005**, *38*, 6352–6366.
- (23) Purmova, J.; Pauwels, K. F. D.; Agostini, M.; Bruinsma, M.; Vorenkamp, E. J.; Schouten, A. J.; Coote, M. L. *Macromolecules* **2008**, *41*, 5527–5539.
- (24) Van Cauter, K.; Van Speybroeck, V.; Waroquier, M. *Macromolecules* **2007**, *40*, 1321–1331.
- (25) Degirmenci, I.; Avci, D.; Aviyente, V.; Van Cauter, K.; Van Speybroeck, V.; Waroquier, M. *Macromolecules* **2007**, *40*, 9590–9602.
- (26) (a) Pross, A.; Shaik, S. *Acc. Chem. Res.* **1983**, *16*, 363–370. (b) Pross, A.; Yamataka, H.; Nagase, S. *J. Phys. Org. Chem.* **1991**, *4*, 135–140.
- (27) Cole, S. J.; Kirwan, J. N.; Roberts, B. P.; Willis, C. R. *J. Chem. Soc., Perkin Trans. 1* **1991**, 103–112.
- (28) Reid, D. L.; Armstrong, D. A.; Rauk, A.; Von Sonntag, K. *Phys. Chem. Chem. Phys.* **2003**, *5*, 3994–3999.
- (29) Beare, K. D.; Coote, M. L. *J. Phys. Chem. A* **2004**, *108*, 7211–7221.
- (30) Rong, X. X.; Pan, H.; Dolbier, W. R. *J. Am. Chem. Soc.* **1994**, *116*, 4521–4522.
- (31) *Handbook of Radical Polymerization*; Matyjaszewski, K., Davis, T. P., Eds.; Wiley-Interscience: Hoboken, NJ, 2002.
- (32) Atkins, P.; de Paula, J. *Atkins' Physical Chemistry*, 8th ed.; Oxford University Press: New York, 2006.
- (33) Frisch, M. J.; Trucks, G. W.; Schlegel, H. B.; Scuseria, G. E.; Robb, M. A.; Cheeseman, J. R.; Montgomery, J. A., Jr.; Vreven, T.; Kudin, K. N.; Burant, J. C.; Millam, J. M.; Iyengar, S. S.; Tomasi, J.; Barone, V.; Mennucci, B.; Cossi, M.; Scalmani, G.; Rega, N.; Petersson, G. A.; Nakatsuji, H.; Hada, M.; Ehara, M.; Toyota, K.; Fukuda, R.; Hasegawa, J.; Ishida, M.; Nakajima, T.; Honda, Y.; Kitao, O.; Nakai, H.; Klene, M.; Li, X.; Knox, J. E.; Hratchian, H. P.; Cross, J. B.; Bakken, V.; Adamo, C.; Jaramillo, J.; Gomperts, R.; Stratmann, R. E.; Yazyev, O.; Austin, A. J.; Cammi, R.; Pomelli, C.; Ochterski, J. W.; Ayala, P. Y.; Morokuma, K.; Voth, G. A.; Salvador, P.; Dannenberg, J. J.; Zakrzewski, V. G.; Dapprich, S.; Daniels, A. D.; Strain, M. C.; Farkas, O.; Malick, D. K.; Rabuck, A. D.; Raghavachari, K.; Foresman, J. B.; Ortiz, J. V.; Cui, Q.; Baboul, A. G.; Clifford, S.; Cioslowski, J.; Stefanov, B. B.; Liu, G.; Liashenko, A.; Piskorz, P.; Komaromi, I.; Martin, R. L.; Fox, D. J.; Keith, T.; Al-Laham, M. A.; Peng, C. Y.; Nanayakkara, A.; Challacombe, M.; Gill, P. M. W.; Johnson, B.; Chen, W.; Wong, M. W.; Gonzalez, C.; Pople, J. A. *Gaussian 03*, revision D.01; Gaussian, Inc.: Wallingford, CT, 2004.
- (34) Degirmenci, I.; Aviyente, V.; Van Speybroeck, V.; Waroquier, M. *Macromolecules* **2009**, *42*, 3033–3041.
- (35) (a) Van Cauter, K.; Van Speybroeck, V.; Vansteenkiste, P.; Reyniers, M. F.; Waroquier, M. *ChemPhysChem* **2006**, *7*, 131–140. (b) Speybroeck, V.; Van Cauter, K.; Coussens, B.; Waroquier, M. *ChemPhysChem* **2005**, *6*, 180–189.
- (36) (a) Gomez-Balderas, R.; Coote, M. L.; Henry, D. J.; Radom, L. *J. Phys. Chem. A* **2004**, *108*, 2874–2883. (b) Coote, M. L. *J. Phys. Chem. A* **2004**, *108*, 3865–3872.
- (37) Smith, D. M.; Nicolaides, A.; Golding, B. T.; Radom, L. *J. Am. Chem. Soc.* **1998**, *120*, 10223–10233.
- (38) Zhao, Y.; Truhlar, D. G. *J. Phys. Chem. A* **2004**, *108*, 6908–6918.
- (39) Zhao, Y.; Schultz, N. E.; Truhlar, D. G. *J. Chem. Theory Comput* **2006**, *2*, 364–382.
- (40) (a) Van Speybroeck, V.; Van Neck, D.; Waroquier, M.; Wauters, S.; Saey, M.; Marin, G. B. *J. Phys. Chem. A* **2000**, *104*, 10939–10950. (b) Sabbe, M. K.; Vandeputte, A. G.; Reyniers, M. F.; Van Speybroeck, V.; Waroquier, M.; Marin, G. B. *J. Phys. Chem. A* **2007**, *111*, 8416–8428.
- (c) Van Cauter, K.; Hemelsoet, K.; Van Speybroeck, V.; Reyniers, M. F.; Waroquier, M. *Int. J. Quantum Chem.* **2005**, *102*, 454–460.
- (41) (a) Hemelsoet, K.; Van Speybroeck, V.; Moran, D.; Marin, G. B.; Radom, L.; Waroquier, M. *J. Phys. Chem. A* **2006**, *110*, 13624–13631. (b) Van Speybroeck, V.; Hemelsoet, K.; Minner, B.; Marin, G. B.; Waroquier, M. *Mol. Simul.* **2007**, *33*, 879–887. (c) Vandeputte, A. G.; Sabbe, M. K.; Reyniers, M. F.; Van Speybroeck, V.; Waroquier, M.; Marin, G. B. *J. Phys. Chem. A* **2007**, *111*, 11771–11786.
- (42) Coote, M. L.; Collins, M. A.; Radom, L. *Mol. Phys.* **2003**, *101*, 1329–1338.
- (43) Wigner, E. Z. *Phys. Chem. B* **1932**, *19*, 203.
- (44) Eckart, C. *Phys. Rev.* **1930**, *35*, 1303–1309.
- (45) Hemelsoet, K.; Van Speybroeck, V.; Waroquier, M. *ChemPhysChem* **2008**, *9*, 2349–2358.
- (46) Da Silva, G.; Chen, C.; Bozzelli, J. W. *Chem. Phys. Lett.* **2006**, *424*, 42–45.
- (47) *CRC Handbook of Chemistry and Physics*, Lide, D. R., Ed.; CRC Press: Boca Raton, FL, 1990–1991.
- (48) Blanksby, S. J.; Ellison, G. B. *Acc. Chem. Res.* **2003**, *36*, 255–263.
- (49) (a) Tomasi, J.; Mennucci, B.; Cancès, E. *THEOCHEM* **1999**, *464*, 211–226. (b) Cancès, M. T.; Mennucci, B.; Tomasi, J. *J. Chem. Phys.* **1997**, *107*, 3032–3041. (c) Mennucci, B.; Tomasi, J. *J. Chem. Phys.* **1997**, *106*, 5151–5158. (d) Mennucci, B.; Cancès, E.; Tomasi, J. *J. Phys. Chem. B* **1997**, *101*, 10506–10517.
- (50) Liptak, M. D.; Gross, K. G.; Seybold, P. G.; Feldgus, S.; Shields, G. C. *J. Am. Chem. Soc.* **2002**, *124*, 6421–6427.
- (51) Olaj, O. F.; Vana, P.; Zoder, M.; Kornherr, A.; Zifferer, G. *Macromol. Rapid Commun.* **2000**, *21*, 913–920.
- (52) Willemsse, R. X. E.; StAM, B. B. P.; Van Herk, A. M.; Pierik, S. C. J.; Klumperman, B. *Macromolecules* **2003**, *36*, 9797–9803.
- (53) Olaj, O. F.; Zoder, M.; Vana, P.; Kornherr, A.; Schnöll-Bitai, I.; Zifferer, G. *Macromolecules* **2005**, *38*, 1944–1948.
- (54) Heuts, J. P. A.; Gilbert, R. G.; Radom, L. *J. Phys. Chem.* **1996**, *100*, 18997–19006.
- (55) Izgorodina, E. I.; Coote, M. L. *Chem. Phys.* **2006**, *324*, 96–110.
- (56) Dedy, M.; Mau, A. W. H.; Moad, G.; Spurling, T. H. *Makromol. Chem.* **1993**, *194*, 1691–1705.
- (57) Coote, M. L.; Davis, T. P. *Macromolecules* **1999**, *32*, 5270–5276.
- (58) Boutevin, B. *J. Polym. Sci., Part A: Polym. Chem.* **2000**, *38*, 3235–3243.
- (59) Odian, G. *Principles of Polymerization*; Wiley-Interscience: New York, 1991.
- (60) Mortimer, G. A. *J. Polym. Sci., Part A: Polym. Chem.* **1966**, *4*, 881–900.
- (61) Atadinc, F.; Selcuki, C.; Sarı, L.; Aviyente, V. *Phys. Chem. Chem. Phys.* **2002**, *4*, 1797–1806.
- (62) McGivern, S. W.; Derecskei-Kovacs, A.; North, S. W.; Francisco, J. S. *J. Phys. Chem. A* **2000**, *104*, 436–442.
- (63) Vijayalakshmi, N.; Reddy, M.; Naidu, S. V.; Ramanjappa, T.; Appalanaidu, P. *Int. J. Polym. Mater.* **2008**, *57*, 709–716.
- (64) Evans, M. A.; Polanyi, M. *Trans. Faraday Soc.* **1938**, *34*, 11–29.
- (65) Chang, Q.; Hao, X.; Duan, L. *J. Hazard. Mater.* **2008**, *159*, 548–553.
- (66) Sojka, R.; Bjorneberg, D.; Entry, J. A. *Adv. Agron.* **2007**, *92*, 75–162.
- (67) Patrick, T. *Semin. Cut. Med. Surg.* **2004**, *23*, 233–235.
- (68) Ravindra, S.; Mohan, Y. M.; Varaprasad, K. *Int. J. Polym. Mater.* **2009**, *58*, 278–296.
- (69) Ehrbar, M.; Schoenmakers, R.; Christen, E. *Nat. Mater.* **2008**, *7*, 800–804.
- (70) Kotaro, S.; Kamigaito, M. *Chem. Rev.* **2009**, *109*, 5120–5156.
- (71) Izgorodina, E. I.; Brittain, D. R. B.; Hodgson, J. L.; Krenske, E. H.; Lin, C. Y.; Namazian, M.; Coote, M. L. *J. Phys. Chem.* **2007**, *111*, 10754–10768.
- (72) Zhao, Y.; Truhlar, D. G. *J. Phys. Chem. A* **2008**, *112*, 1095–1099.
- (73) Brittain, D. R. B.; Lin, C. Y.; Gilbert, A. T. B.; Izgorodina, E. I.; Gill, P. M. W.; Coote, M. L. *Phys. Chem. Chem. Phys.* **2009**, *11*, 1138–1142.
- (74) Pross, A. *Theoretical and Physical Principles of Organic Reactivity*; Wiley-Interscience: New York, 1995.
- (75) Hansch, C.; Leo, A.; Taft, R. W. *Chem. Rev.* **1991**, *91*, 165–195.
- (76) Coote, M. L.; Davis, T. P. *Macromolecules* **1999**, *32*, 4290–4298.